AGU PUBLICATIONS

JGR

Journal of Geophysical Research: Atmospheres

RESEARCH ARTICLE

10.1002/2013JD020272

Key Points:
- Observed tropical convection with CloudSat data
- Convection invigorated with increased aerosol optical depth
- Trends were statistically significant

Correspondence to:
R. L. Storer,
storer@uwm.edu

Citation:
Storer, R. L., S. C. van den Heever, and T. S. L'Ecuyer (2014), Observations of aerosol-induced convective invigoration in the tropical east Atlantic, *J. Geophys. Res. Atmos.*, *119*, 3963–3975, doi:10.1002/2013JD020272.

Received 31 MAY 2013
Accepted 8 MAR 2014
Accepted article online 13 MAR 2014
Published online 2 APR 2014

Observations of aerosol-induced convective invigoration in the tropical east Atlantic

R. L. Storer[1], S. C. van den Heever[2], and T. S. L'Ecuyer[3]

[1]Department of Mathematical Sciences, University of Wisconsin-Milwaukee, Milwaukee, Wisconsin, USA, [2]Department of Atmospheric Science, Colorado State University, Fort Collins, Colorado, USA, [3]Department of Atmospheric and Oceanic Sciences, University of Wisconsin-Madison, Madison, Wisconsin, USA

Abstract Four years of CloudSat data have been analyzed over a region of the east Atlantic Ocean in order to examine the influence of aerosols on deep convection. The satellite data were combined with information about aerosols taken from the Global and Regional Earth-System Monitoring Using Satellite and In Situ Data model. Only those profiles fitting the definition of deep convective clouds were analyzed. Overall, the cloud center of gravity, cloud top, and rain top were all found to increase with increased aerosol loading. These effects were largely independent of the environment, and the differences between the cleanest and most polluted clouds sampled were found to be statistically significant. When examining an even smaller subset of deep convective clouds likely to be part of the convective core, similar trends were seen. These observations suggest that convective invigoration occurs with increased aerosol loading, leading to deeper, stronger storms in polluted environments.

1. Introduction

While increasing research has been performed in order to address the problem of aerosol impacts on deep convection, many questions still remain unanswered. Several studies [*Andreae et al.*, 2004; *Khain et al.*, 2005; *Koren et al.*, 2005; *van den Heever et al.*, 2006; *van den Heever and Cotton*, 2007; *Lee et al.*, 2008a; *Li et al.*, 2008; *Rosenfeld et al.*, 2008; *Lebo and Seinfeld*, 2011; *van den Heever et al.*, 2011; *Storer and van den Heever*, 2013; *Fan et al.*, 2013] suggest that increased aerosol concentrations will lead to the invigoration of deep convective storms; however, there is still no clear consensus on this effect, as recently summarized in *Tao et al.* [2012]. It is generally established that in a polluted environment, or one which contains higher number concentrations of aerosols that can act as cloud condensation nuclei (CCN), collision and coalescence in deep convective systems will be less effective due to the increased numbers of smaller cloud droplets, thus leading to a reduction in warm rain production. This leaves higher amounts of liquid water in cloud that can be lofted to form ice, providing an additional source of latent heating which can increase the buoyancy of an updraft. These changes can lead to stronger storms with higher cloud tops, greater ice mass, and heavier surface precipitation [*Andreae et al.*, 2004; *Khain et al.*, 2005; *Koren et al.*, 2005; *van den Heever et al.*, 2006; *Li et al.*, 2008; *Rosenfeld et al.*, 2008; *Storer et al.*, 2010; *Tao et al.*, 2012; *Storer and van den Heever*, 2013].

Changes in deep convective properties can have important impacts on both the local and the large scale. On short temporal and spatial scales, the higher precipitation rates associated with more vigorous convection are of great concern. In terms of larger scale impacts, *Fan et al.* [2012] describe how invigoration of deep convection can lead to changes in weather patterns, from the smaller scale (e.g., sea-breeze circulations) up to monsoons and even the Hadley circulation, through warming at the top of the atmosphere. *Van den Heever et al.* [2011] demonstrated that convective invigoration may lead to increases in midlevel and high clouds at the expense of low clouds through changes in convective circulations. In addition, changes to the microphysical properties of cloud droplets and ice crystals, alone or in combination with convective invigoration, can lead to differences in high cloudiness [*Fan et al.*, 2013], which would have important implications when considering the radiation budget of the atmosphere.

Typical measurement techniques which give us information about such properties as aerosol optical depth often cannot measure these quantities when clouds are present, making it a challenge to obtain collocated measurements of aerosols with deep convective storms. However, a few observational studies do exist that support the theory of convective invigoration suggested by modeling efforts. Some of the first observational evidence of convective invigoration was seen by *Andreae et al.* [2004] in their study of convection

over the Amazon during the biomass burning season. The authors discovered strong thunderstorms with enhanced ice processes and heavy rain showers during smoke events, more so than when the environment was less polluted by smoke aerosols. Since then others [e.g., *Lin et al.*, 2006; *Ten Hoeve et al.*, 2012] have also found evidence of higher cloud tops, enhanced heavy precipitation, and increased ice amounts in the same region. Similar evidence has also been found for convective invigoration (e.g., increased cloud tops, more frequent lightning, and heavier precipitation events) in polluted environments over the North Atlantic Ocean [*Koren et al.*, 2005], in the southeast United States [*Bell et al.*, 2008], and in China [*Wang et al.*, 2011]. *Wang et al.* [2009] analyzed both observational and modeling data and found evidence that smoke from biomass burning in Central America may lead to an enhancement of severe weather in the south central United States. *Heiblum et al.* [2012] recently performed an observational study examining satellite data over several regions across the globe. They found evidence of convective invigoration in many of the regions studied in the form of an increased rain center of gravity. In another study [*Li et al.*, 2011], a 10 year data set over the Southern Great Plains in the United States was used to demonstrate that low-based, mixed-phase clouds (i.e., summer deep convective clouds (or DCCs)) show evidence of convective invigoration when aerosol concentrations are higher.

The goal of this study is to examine a large sample of observed tropical deep convective clouds developing under a range of aerosol concentrations in order to search for evidence of convective invigoration with increased aerosols. We do not seek to define the processes responsible for convective invigoration but simply to examine whether observational evidence exists of some of the fundamental differences in convective storms that have been seen in previous studies in association with enhanced aerosol concentrations [*Andreae et al.*, 2004; *Khain et al.*, 2005; *van den Heever et al.*, 2006; *Rosenfeld et al.*, 2008; *Khain*, 2009; *van den Heever et al.*, 2011; *Storer and van den Heever*, 2013; *Fan et al.*, 2013]. We utilize satellite observations of deep convective clouds from the CloudSat Cloud Profiling Radar, in combination with the output from a global transport model used as a proxy for aerosol loading, in order to look for evidence of convective invigoration. The use of CloudSat data provides a unique opportunity to examine aerosol impacts on deep convection because of the global coverage of the satellite and the ability of the radar to penetrate clouds, thereby offering information about the vertical structure of convective systems. In keeping with previous studies, we will show that occurrences of deep convection in more polluted environments do have greater reflectivity throughout the column and that the clouds are more vertically developed. We suggest that these changes are observational evidence of convective invigoration.

2. Data and Methods

Observations of deep convection were obtained from the CloudSat Cloud Profiling Radar (CPR) [*Stephens et al.*, 2002]. The CPR is a 94 GHz nadir-looking radar with a vertical gate spacing of 240 m. The horizontal resolution is 1.4 km (cross track) × 1.8 km (along track). The high frequency of this radar makes it very sensitive to the presence of cloud and ice particles (the minimum detectable signal is about −30 dBZ). Reflectivity data used in this study are obtained from the level-2 product 2B-GEOPROF [*Mace et al.*, 2007], which provides vertical profiles of reflectivity corrected for gaseous attenuation. The 2B-GEOPROF product also provides a cloud mask for use in defining where cloud is present.

For the purposes of this study, only profiles selected as "Deep Convective Clouds" (DCCs) were analyzed. A DCC was defined where the depth of continuous cloud (as established by the CPR Cloud Mask product) was at least 8 km and is similar to that used in the modeling study of *Storer and van den Heever* [2013]. The choice of 8 km depth was arbitrary, but it is large enough to rule out the majority of cumulus congestus clouds, while still being shallow enough to allow for profiles in the core of deep convective storms, where the base measured by the CPR may be artificially high due to radar attenuation. These DCCs do not represent separate clouds but rather are individual profiles measured by the CPR, many of which may be present in an individual deep convective storm. The sample of DCCs may consist of both the convective core of storms as well as regions of deep, more stratiform-like cloud.

Four years (2006–2009) of CloudSat data (both ascending and descending overpasses) were analyzed over a region of the east Atlantic bounded by 0–40°N and 0–40°W. In order to avoid differences due to land-based versus oceanic convection, only deep convective profiles over the ocean were used. This region of the east Atlantic was chosen due to the frequent dust events that occur off the west coast of Africa within the Saharan Air Layer (SAL) [*Carlson and Prospero*, 1972; *Zipser et al.*, 2009]. In addition, much of the aerosol

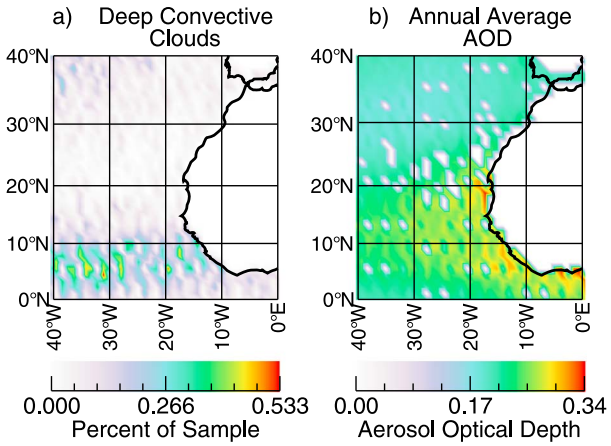

Figure 1. (a) The frequency of occurrence of deep convective clouds seen by CloudSat in the years 2006–2009 and (b) aerosol optical depth from GEMS model output, matched to CloudSat data and averaged over the 4 year period of study. A wave-like pattern can be seen in both plots due to the location of CloudSat overpasses. GEMS = Global and Regional Earth-System Monitoring Using Satellite and In Situ Data

present in this region is likely to be composed of dust and sulfate [*Zipser et al.*, 2009], similar to that modeled in *Storer and van den Heever* [2013]. Shown in Figure 1a is the frequency of occurrence of DCCs in the region. The percent of the total sample located in a 1° by 1° box is contoured. A majority of the DCCs analyzed are located in the lower latitudes and are associated with the Intertropical Convergence Zone. The locations of more frequent DCCs align well with what is shown in *Liu et al.* [2007], although it should be noted that cloud fraction is not the variable shown here.

In order to examine aerosol indirect effects on these DCCs, a large, consistent record of aerosol measurements was required. Satellite aerosol optical depth (AOD) measurements collocated with deep convection are difficult to obtain, as most aerosol algorithms require an absence of cloud and few in situ data exist over the ocean. For these reasons, output from a global transport model was used to determine if a DCC developed in a polluted or clean environment. The Global and Regional Earth-System Monitoring Using Satellite and In Situ Data (GEMS) project (http://gems.ecmwf.int) [*Hollingsworth et al.*, 2008] utilizes data assimilation of aerosol emissions inventories and satellite data, in combination with the European Centre for Medium-Range Weather Forecasts (ECMWF) model, in order to provide detailed global coverage of chemical and aerosol species. The use of data assimilation in the analysis provides improved AOD information as compared to the model alone and allows for gaps in satellite data to be filled in [*Benedetti et al.*, 2009]. The GEMS project provides model-simulated 550 nm AOD, representing what might be observed by a sensor such as MODIS (Moderate Resolution Imaging Spectroradiometer) [*Remer et al.*, 2005], in the absence of cloudiness. For a sense of the typical GEMS AOD in the region, Figure 1b is a contour plot showing all samples falling within each 1° by 1° box, averaged spatially and temporally for the entire 4 year time period analyzed here.

A center of gravity (COG) was calculated for each profile utilizing a technique similar to that described by *Koren et al.* [2009] and used by *Heiblum et al.* [2012]; however, instead of rain rate, the COG was calculated using values of reflectivity, as shown below.

$$\mathrm{COG} = \frac{\sum_i Z_i H_i}{\sum_i Z_i} \tag{1}$$

In this equation, Z is the measured reflectivity and H is the height in meters of each level, i. The sums performed in the calculation of COG were started at the level of maximum reflectivity, rather than the surface, in order to reduce the possibility that attenuated profiles were affecting the results. Generally, a higher COG is present where values of reflectivity are greater, or more condensate is present at higher levels of the cloud.

Other parameters analyzed include cloud top, the highest level containing cloud as defined by the CPR Cloud Mask, and rain top, the highest level where the reflectivity has a value of at least 0 dBZ. To learn something of the microphysical characteristics of these clouds, ice water content was obtained from the CloudSat Level 2 data product 2B-CWC-RO [*Austin et al.*, 2009]. The ice water content was vertically integrated to create ice water path.

As previous work has found that aerosol indirect effects can differ depending on environmental parameters such as convective available potential energy (CAPE) [e.g., *Storer et al.*, 2010] and lower tropospheric static stability (LTSS) [e.g., *Matsui et al.*, 2004], it was useful to separate the aerosol trends found here by environmental regimes. Environmental variables were calculated using information from the ECMWF-AUX product,

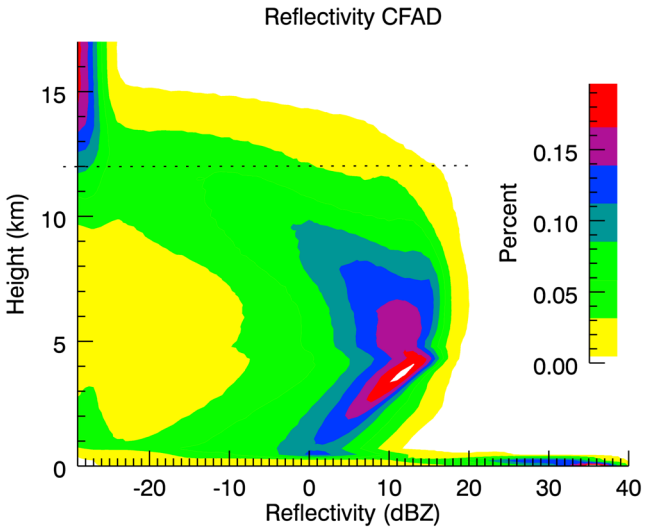

Figure 2. A contoured frequency by altitude diagram (CFAD), showing the frequency of occurrence of values of reflectivity at different heights for the total sample of deep convective clouds sampled in this study. Data are binned at 1 dBZ intervals at each level and then normalized by the total number of samples in that level. The mean cloud top (~12 km) is noted, and above that, reflectivity values are mostly at or below the minimum detectable threshold.

and CAPE and LTSS (simply the lapse rate between the surface and the 700 mb level) were used to separate environmental impacts from those of aerosols on convective storms.

3. Results

3.1. General Statistics

Over a quarter of a million DCCs (~3.5e5) were analyzed over the 4 year period. As explained in section 2, DCCs are those profiles with cloud present through a depth of at least 8 km. For a sense of what these DCC reflectivity profiles look like, Figure 2 shows a contoured frequency by altitude diagram (CFAD) [*Yuter and Houze*, 1995] of the entire sample of DCCs analyzed in this study. The samples were binned by 1 dBZ at each level and then normalized by the total number of samples at that level. The average cloud top of the DCCs analyzed is just over 12 km; above this, the majority of the DCCs have reflectivity values near or below the minimum detectable signal. Moving downward through the troposphere, the reflectivity quickly increases as the CPR detects ice particles in the upper levels of the DCCs. Nearly all of the profiles sampled have a maximum reflectivity greater than 0 dBZ, which is often considered the threshold for precipitation-sized particles [*Haynes et al.*, 2009], and a large number reach 15 dBZ, signifying great amounts of condensate present. An increase in reflectivity associated with the melting level is clearly visible near 4 km above ground level, and below that the reflectivity decreases rapidly toward the surface as the radar signal becomes attenuated due to heavy precipitation.

The AOD estimated in the geographic region studied here ranged between 0.03 and 1.64 during the time period studied, with an area and time average of 0.23. A histogram of AOD for the profiles analyzed is shown in Figure 3. The AOD is widely variable over the region and time period studied here and is similar to histograms shown in *Remer et al.* [2008]. Also indicated in Figure 3 are divisions denoting 10 equal sample size bins. That is, each bin contains 10% of the DCCs, or about 3.5e4 sample profiles. The cleanest 10% of the samples have an average AOD of 0.1, while the most polluted 10% have AOD averaging near 0.9. Aerosol climatologies such as described in *Remer et al.* [2008] have shown that remote ocean regions typically have average AOD on the order of 0.1, while strongly polluted regions such as the Amazon during the biomass burning season have average values of AOD approaching 1. As is evident from Figure 3, the AOD in the east

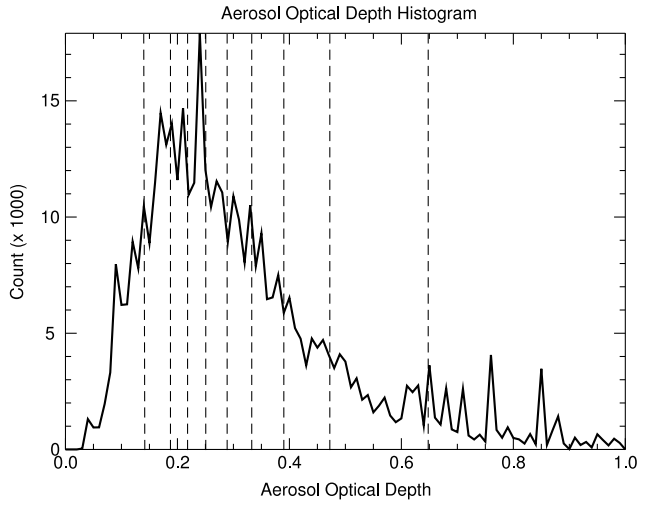

Figure 3. A histogram showing the frequency of occurrence of values of aerosol optical depth sampled from the GEMS data set. Vertical dashed lines denote the divisions between bins each containing 10% (~3.5e4 samples) of the data.

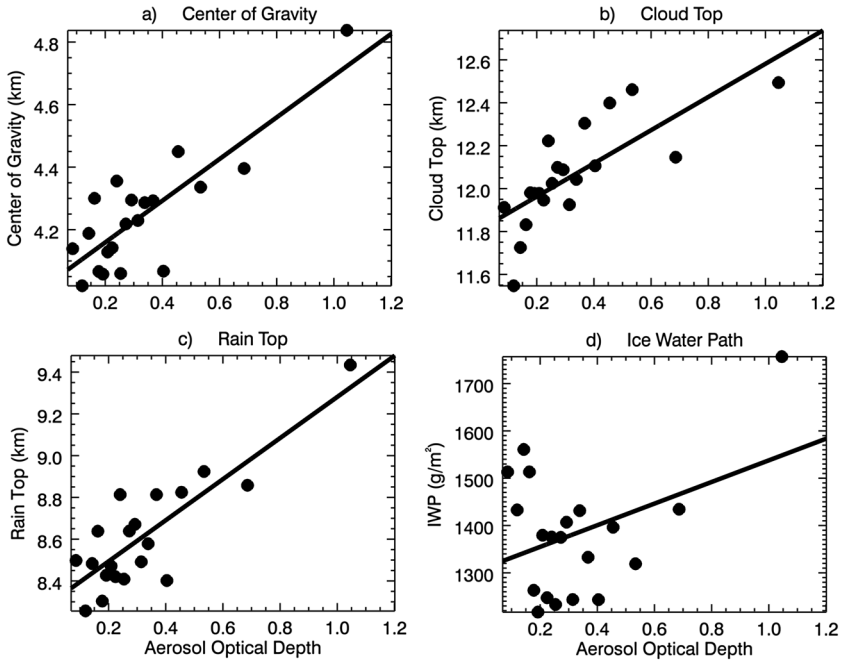

Figure 4. Average values of (a) center of gravity, (b) cloud top, (c) rain top, and (d) ice water path. Symbols denote 20 bins each containing ~1.75e4 samples, while the trend lines were calculated using ordinary least squares with 50 bins of ~7000 samples each.

Atlantic region encompasses this entire range, though the majority of DCCs sampled here have AOD values that fall within a more "moderate" range of 0.2–0.4.

Shown in Figure 4 are the four DCC properties analyzed, plotted as a function of AOD. For this plot, the data were split into 20 equal sample size bins (each containing ~1.75e4 DCC profiles) based on the AOD, and the average of each DCC parameter was calculated within each aerosol bin. Additionally, a trend line was calculated for each parameter, using ordinary least squares with the data split into 50 bins. This trend line is plotted for demonstrative purposes, as it is not relevant to the statistical analysis described later in this section; however, the trend line is not sensitive to the number of bins used. The first DCC property analyzed here is the center of gravity, as defined in section 2. The COG represents both the magnitude of reflectivity values and how high they reach in the troposphere. Figure 4a shows that there is a clear upward trend in COG with increasing AOD. Higher values of COG can result from clouds with greater vertical extent and/or clouds containing more condensate aloft, both of which have been seen in polluted storms (as summarized in *Tao et al.* [2012]). Larger vertical extent would suggest possible convective invigoration, as seen previously [*Andreae et al.*, 2004; *Khain et al.*, 2005; *Koren et al.*, 2005; *van den Heever et al.*, 2006; *van den Heever and Cotton*, 2007; *Lee et al.*, 2008a; *Rosenfeld et al.*, 2008; *Lebo and Seinfeld*, 2011; *Storer and van den Heever*, 2013]. Many studies [e.g., *Lynn et al.*, 2005; *Khain et al.*, 2005; *van den Heever et al.*, 2006; *Lee et al.*, 2008a; *Storer et al.*, 2010; *Storer and van den Heever*, 2013] have also noted that increased aerosol loading leads to enhanced ice and liquid amounts in deep convective clouds. In addition, *Heiblum et al.* [2012] observed increased values of COG with increased aerosols in their study utilizing TRMM data.

In order to assess possible reasons for the increase in COG with increased aerosol loading, Figure 4 also demonstrates the trends in cloud top, rain top (0 dBZ echo height), and ice water path. Cloud top and rain top show clear increases with enhanced aerosol optical depth, which suggests that convective invigoration may be occurring with higher values of AOD. This signal of increased cloud and rain top would appear to be in keeping with results from previous studies (as discussed above) that found deeper, stronger storms in more polluted simulations.

The ice water path shows a weakly positive trend with increased aerosol loading. Based on previous modeling studies [*Lynn et al.*, 2005; *Khain et al.*, 2005; *van den Heever et al.*, 2006, 2011; *Rosenfeld et al.*, 2008; *Storer et al.*, 2010; *Storer and van den Heever*, 2013; *Fan et al.*, 2013], we would expect an increase in cloud ice with

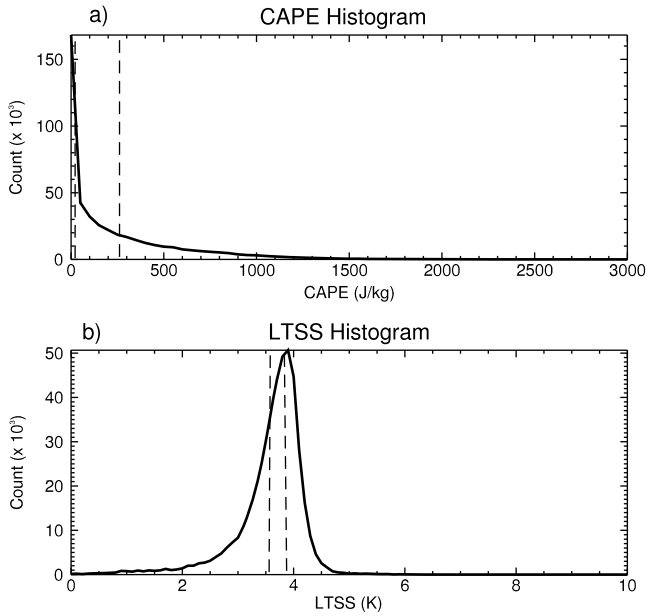

Figure 5. Histograms showing the frequency of occurrence of (a) convective available potential energy (CAPE) and (b) lower tropospheric static stability (LTSS) calculated using ECMWF-AUX data. Vertical dashed lines denote the divisions between high (greater than 250 J/kg for CAPE or 3.95 K for LTSS), medium, and low (less than 38 J/kg for CAPE or 3.67 K for LTSS) values for each environmental parameter.

increased aerosol amounts. However, there is some uncertainty associated with the values of ice water path due to the fact that radar-based retrievals of ice water content are sensitive to the choice of the size and density parameters used [*Protat et al.*, 2009]. Changes in aerosol concentration can also affect the size of ice particles, and so competing effects may be leading to the lack of a consistent trend.

3.2. Environmental Dependence

As mentioned in section 2, the net effect of aerosols on convection can depend strongly on the environment, and thus, the DCCs analyzed were separated by environmental parameters in an attempt to isolate the signal attributable to aerosol loading from that due to environmental forcing. There are a number of parameters that can be a factor; however, we chose two common stability parameters (CAPE and LTSS) to analyze here. Both parameters are indicative of the dynamic forcing that would affect the DCC parameters in the absence of differences in aerosol forcing. CAPE is a measure of the energy available for a convective updraft to utilize as it grows, and higher values indicate the possibility of stronger updrafts and more intense convection. LTSS describes the stability in the boundary layer. Higher values of LTSS indicate a capping inversion which can act to prevent deep convection from forming. Histograms of CAPE and LTSS for the region and time period analyzed here are shown in Figure 5. The total sample was sorted by CAPE (LTSS) and then divided into three bins with the same number of samples in each bin. These bins were then considered to be low, medium, and high CAPE (LTSS), and the divisions between these CAPE (LTSS) bins were used within each aerosol bin. The same four DCC characteristics discussed previously are plotted in Figure 6, thresholded by high, medium, and low CAPE regimes. It is clear that all four properties increase with increasing CAPE. This is not surprising, as higher values of CAPE are typically associated with stronger, more vertically developed storms, which would also produce more ice. Aerosol-induced increasing trends in COG, cloud top, rain top, and ice water path generally hold for all the CAPE environments. Similar to the results seen in *Storer et al.* [2010], CAPE is the dominating factor when determining these properties, yet the aerosol loading has a notable effect. The trends are generally clearer for low and medium CAPE, which is also in keeping with *Storer et al.* [2010], who noted decreased impacts of aerosols for storms in the most unstable environments. While the effects of convective invigoration are still evident for the most favorable storm environments (i.e., those with the highest CAPE), aerosols generally have a more pronounced impact in low CAPE environments that only support weaker storms.

Figure 7 demonstrates that results are similar when DCCs are separated by LTSS rather than CAPE. Though not as clear as with CAPE, the four properties examined here (COG, cloud top, rain top, and ice water path) all generally increase with increasing LTSS. This is because the LTSS sampled here is generally quite low compared to what is seen in other parts of the world [*Matsui et al.*, 2004]. Very low values of LTSS will be associated with widespread convection that may be weaker, as the boundary layer offers no resistance to upward motion. Slightly higher values of LTSS may indicate sufficient stability to prevent widespread convection, thereby only allowing for stronger convection to penetrate the boundary layer (similar to the concept of convective inhibition or CIN). Regardless of the value of LTSS, the DCC characteristics demonstrate the same generally increasing trends of COG, cloud top height, rain top height, and ice water path with increased AOD.

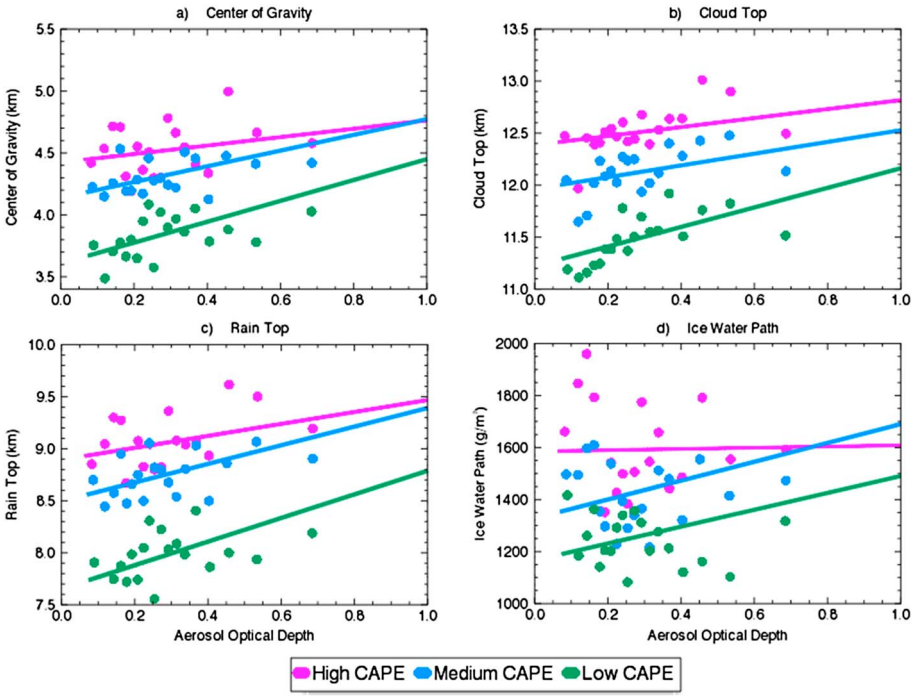

Figure 6. Average values of (a) center of gravity, (b) cloud top, (c) rain top, and (d) ice water path for each aerosol bin. Deep convective clouds are split by high (greater than 250 J/kg), medium, and low (less than 39 J/kg) CAPE. Symbols denote 20 bins each containing ~5e3 samples, while the trend lines were calculated using ordinary least squares with 50 bins of ~2500 samples each.

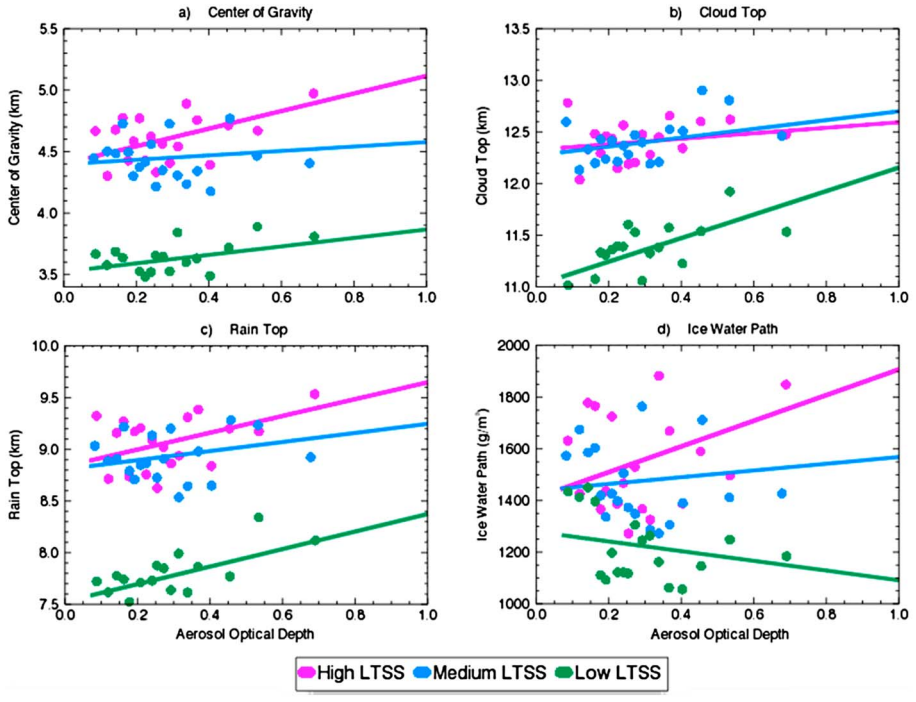

Figure 7. As in Figure 6, but profiles are split up by high (greater than 3.95 K), medium, and low (less than 3.67 K) LTSS.

Table 1. Spearman's Rank Correlation Coefficients for Each Sample With Aerosol Optical Depth[a]

	COG (m)	Cloud Top (m)	Rain Top (m)	Ice Water Path (g/m^2)
All DCCs	**0.056**	**0.112**	**0.075**	**−0.005**
High CAPE	**0.031**	**0.081**	**0.051**	**−0.011**
Medium CAPE	**0.049**	**0.089**	**0.067**	**−0.009**
Low CAPE	**0.062**	**0.128**	**0.075**	**−0.014**
High LTSS	**0.065**	**0.035**	**0.063**	**0.032**
Medium LTSS	−0.003	**0.063**	**0.018**	**−0.016**
Low LTSS	**0.028**	**0.129**	**0.052**	**−0.06**

[a]Values that are significant at the 95% level are in bold.

3.3. Statistical Significance

While the trends in the four parameters analyzed here are relatively clear from a subjective standpoint, it is evident from the figures described above that there is quite a bit of noise in the data, particularly in the moderate AOD range of 0.2–0.4. *Storer and van den Heever* [2013] also found strong relationships when considering very clean and very polluted conditions but saw increased variability in the aerosol response for moderately polluted conditions. This noise may be due to many factors, including competing microphysical and dynamic effects, or the fact that we are sampling convection at different stages in its life cycle. In order to objectively determine whether the aerosol effect is indeed significant, two different statistical tests were performed on each sample of DCCs (a sample being all DCCs, only those with high CAPE, etc.).

The first test performed was a calculation of the Spearman rank correlation coefficient [*Wilks*, 2006], a nonparametric method of assessing correlation. Table 1 shows the values of the Spearman correlation coefficient. In bold are the values which are significant at the 95% level. The second test examines the difference between the 10% of each sample of DCCs that contain the lowest values of AOD (the "clean" DCCs, with an average AOD of 0.10) and those with the 10% highest AOD values (the "polluted" DCCs with an average AOD of 0.88). A Wilcoxon-Mann-Whitney rank-sum test was performed to look for a difference in location of the "clean" and "polluted" values of each parameter. If this test shows significance, it means that the "clean" and "polluted" values are more likely to come from different populations. Shown in Table 2 are the differences in the mean between the "polluted" and "clean" samples. Again, the values significant at the 95% level are highlighted in bold. These tests demonstrate that nearly all of the trends discussed are statistically significant and hence cannot simply be attributed to noise in the sample. The differences in COG, cloud top, and rain top are all positive; that is, the average is larger for polluted samples. Many of these differences are larger than 500 m. Also quite clear in both Tables 1 and 2 is the fact that the trends and differences are larger when the CAPE is lower, again consistent with previous studies such as *Storer et al.* [2010]. Ice water path is less consistent than the other parameters, in that both positive and negative trends show significance. Again, it is likely that there are competing microphysical effects that are impacting the ice water content retrieval; hence, these trends may not be realistic.

To visualize the differences due to aerosol effects in a more straightforward way, a CFAD was calculated for the difference between the polluted and clean DCCs (Figure 8a). To create this figure, a CFAD was created for each group of DCCs (the most polluted and the cleanest) and normalized by the total number of samples at

Table 2. Difference Between "Polluted" and "Clean" DCCs for Each Sample[a]

	COG (m)	Cloud Top (m)	Rain Top (m)	Ice Water Path (g/m^2)
All DCCs	**536.7**	**590.5**	**768.9**	**122.5**
High CAPE	**210.8**	**342.7**	**358.0**	**−105.9**
Medium CAPE	**544.6**	**449.5**	**730.8**	**223.9**
Low CAPE	**689.8**	**637.4**	**917.2**	**187.4**
High LTSS	**668.6**	**141.6**	**693.2**	**463.2**
Medium LTSS	**132.2**	**146.9**	**242.9**	−27.5
Low LTSS	228.1	**801.4**	**586.0**	**−262.0**

[a]Values that are significant at the 95% level are in bold.

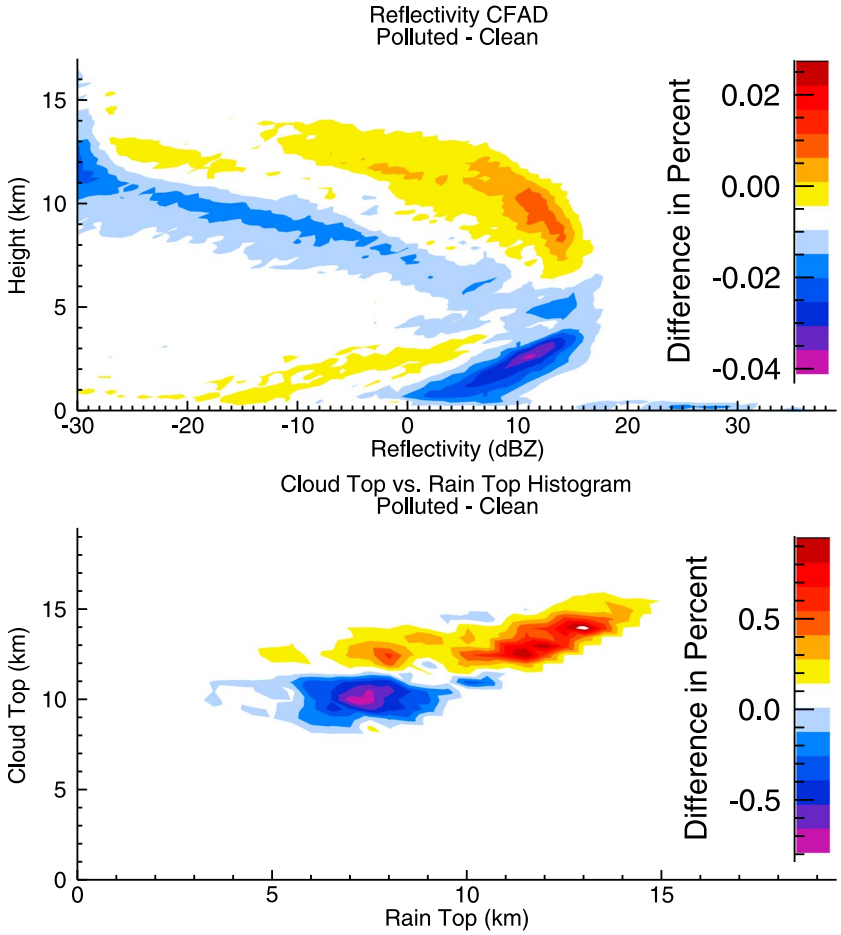

Figure 8. (a) A difference CFAD, calculated by subtracting normalized CFADs from the most polluted and cleanest 10% of the samples. (b) A two-dimensional histogram showing the difference in the frequency of occurrence of values of cloud top and rain top between the polluted and clean samples.

each level before the difference was taken. Since there are such a large number of DCCs analyzed, the percentages contoured are small; however, this plot can help to summarize some of what was seen in Table 2. A visually distinct difference between the clean and polluted samples can be noted here, with a shift toward larger values of reflectivity higher in the atmosphere in the polluted DCCs. This shift is associated with mean values of COG, cloud top, and rain top that differ by over 500 m between the clean and polluted storms. The changes in cloud top and rain top are particularly clear in Figure 8b, which shows a contoured histogram of these two parameters. This difference plot was calculated in a similar manner as the difference CFAD and demonstrates, again, a clear shift toward higher cloud tops and rain tops for those DCCs in the most polluted environments.

3.4. Convective Versus Stratiform Partitioning

It is difficult when analyzing observations to attribute a mechanism to the signals of increased vertical development that we see in this study. The prevailing theory is that of convective invigoration described above; that increased latent heating leads to increased updraft speed, which would explain the higher values of cloud top, rain top, and center of gravity. This theory would suggest that these changes would be particularly noticeable in the convective core, dominated by the storm updraft. However, recently, two studies have shown differences in the response of deep convection to aerosols depending on whether it was the convective core or the surrounding stratiform region that was analyzed. *Min et al.* [2009] looked at a case study of dust affecting a mesoscale convective system in the eastern Atlantic using observations from multiple satellite platforms. They discovered a shift from heavier convective precipitation rates to lighter stratiform rates and evidence of the suppression of convective cores in the polluted part of the storm, counter to what would be expected from the theory of convective invigoration. In a recent modeling study by *Fan*

Table 3. Results When Dividing the Sample Into the Convective Core Versus Stratiform DCCs[a]

	15 dBZ		Congestus	
	Core	Stratiform	Core	Stratiform
COG (m)	**571.0**	**486.8**	**632.5**	**519.2**
	0.128	**0.059**	**0.096**	**0.060**
Cloud Top (m)	**718.5**	**548.9**	**842.0**	**588.9**
	0.150	**0.106**	**0.093**	**0.111**
Rain Top (m)	**743.8**	**731.2**	**856.9**	**757.2**
	0.126	**0.074**	**0.094**	**0.077**
Ice Water Path (g/m^2)	153.4	**24.5**	319.4	**121.0**
	0.005	**0.007**	**−0.019**	−0.001

[a]For each parameter, the first row shows the differences as in Table 2, and the second row the correlations as in Table 1. Values that are significant at the 95% level are in bold.

et al. [2013] the authors examined the response of DCCs to increased aerosols in three regions: southeast China, the southern Great Plains of the United States, and the tropical west Pacific. All three regions showed increased high cloud fraction, cloud top heights, and cloud thickness, whether or not there was evidence of convective invigoration in the form of increased updraft mass flux. The authors suggest that in fact, the changes they saw were largely associated with microphysical differences in the anvil region of the storms, where more ice is detrained from the convective cores and then dissipates more slowly due to the lower fall velocities associated with smaller ice particles. To examine this theory, we look at the response to aerosol loading of those DCCs likely to be a deep convective core with a growing updraft, in comparison to the surrounding deep stratiform clouds.

Without direct observations of updraft speed, it is difficult to determine precisely which DCCs are in a growing convective core. We have chosen to examine two simple metrics to separate the most intense DCC cores from the surrounding, deep stratiform clouds. Differences in the response of these convective cores from the rest of the sample may hint at the physical mechanisms at work in this region. The first selection included DCC profiles with a maximum reflectivity value of at least 15 dBZ, a relatively large reflectivity which suggests enough of an updraft to support large ice particles [*Durden et al.*, 2009]. Only DCCs with the maximum occurring above 5 km were chosen, so as to avoid contamination with the bright band. Of the total DCC profiles, 17% met this criterion. The second selection was similar to that used by *Luo et al.* [2009] to select growing cumulus congestus clouds. For this metric, DCCs were selected as a convective core if the 0 dBZ rain top height was within 1 km of the cloud top height and the 10 dBZ echo top height was within 2 km of the cloud top height. Even fewer DCCs (roughly 0.5% of the total sample) were considered the convective core using this selection criterion. For each metric, those DCCs not categorized as the convective core were classified as part of the deep stratiform region.

For each of the two criteria, the same statistical tests were run for both the core and stratiform DCCs. Results are shown in Table 3. For either selection metric, the core and stratiform regions both demonstrate similar behavior to the entire sample of DCCs as discussed above. Cloud tops, rain tops, and the center of gravity are all substantially increased for polluted DCCs, whether they are a part of the convective core or not, and in fact those DCCs within the convective core show a stronger signal in most cases. The ice water path again does not show a consistent trend, which is even more apparent with the smaller sample sizes. If the data are split up by environmental parameters, the trends remain consistent. Though the microphysical effects described by *Fan et al.* [2013] may certainly be a contributing factor to the changes in DCCs seen here, the differences apparent in the deep convective core between polluted and clean regions suggest that convective invigoration is, in fact, occurring within this region.

4. Discussion

Four years of CloudSat data matched with GEMS model output have been analyzed in a region of the east Atlantic Ocean in order to determine whether there is any observational evidence of aerosol-induced convective invigoration in deep convective clouds. These results support previous observational and modeling

studies [*Andreae et al.*, 2004; *Khain et al.*, 2005; *van den Heever et al.*, 2006; *van den Heever and Cotton*, 2007; *Lee et al.*, 2008a; *Li et al.*, 2008; *Rosenfeld et al.*, 2008; *Lebo and Seinfeld*, 2011; *Li et al.*, 2011; *Storer and van den Heever*, 2013; *Fan et al.*, 2013] showing evidence that increased aerosol concentrations can lead to convective invigoration. These studies are in general agreement that polluted clouds produce less warm rain through the aerosol-induced suppression of the collision and coalescence processes, as the large numbers of small droplets make the warm rain process less efficient. There is then more cloud water remaining in these clouds, which can be lofted to form ice, providing a source of increased latent heating aloft. Additionally, as there are more and smaller hydrometeors in the polluted clouds, the surface area onto which vapor can deposit is increased. Hence, vapor deposition onto both liquid water and ice increases substantially, thereby further increasing the latent heating throughout the cloud [*Storer and van den Heever*, 2013]. The increased buoyancy from latent heating competes with the increased weight of condensate loading in the updraft. *Storer and van den Heever* [2013] found that despite the effects of condensate loading, DCCs in polluted simulations were deeper, wider in horizontal extent, and produced more total precipitation. The fact that observational evidence shown here is in agreement with model simulations of similar clouds and environmental conditions suggests that these mechanisms described by *Storer and van den Heever* [2013] (and also others, as summarized above and by *Tao et al.* [2012]) may explain the evidence of convective invigoration evident in the observations analyzed here.

The east Atlantic region was chosen for this study because of the frequent dust storms that occur off the west coast of Africa, and also for the similarity in environment and aerosol type to that modeled by *Storer and van den Heever* [2013]. Observations of aerosols in this region [e.g., *Zipser et al.*, 2009] show that it is characterized largely by dust, often mixed with sulfate aerosols. Dust particles have been known to act as CCN, giant CCN (GCCN), and ice nuclei (IN) [*DeMott et al.*, 2003; *Twohy et al.*, 2009]. Dust can also absorb solar radiation and act to heat the atmosphere, as is typically seen with aerosols such as black carbon. This heating would generally stabilize the atmosphere and act to suppress convection in what is known as the semi-direct effect; however, due to the selection of only those profiles in which deep convection is already occurring, we are essentially ruling out this effect on individual storms. Therefore, changes in the frequency of occurrence of deep convective clouds, or in large-scale circulation, due to this semi-direct effect, would not be seen with a statistical study such as this.

The results seen here cannot necessarily be extended to other regions of the globe, for two main reasons. Firstly, aerosol composition varies widely with geography [*Remer et al.*, 2008], and so any hypothesis about the effects of dust and sulfate on DCCs in the east Atlantic may not hold when considering other regions where different aerosol types are predominant (e.g., regions of biomass burning). Also, as convection is not identical in character around the world, meteorological impacts on convection may change how it responds to the presence of increased aerosols. For instance, several studies [e.g., *Khain et al.*, 2010; *Storer et al.*, 2010] have shown that strongly forced midlatitude convection may be less likely to undergo convective invigoration. This study may not be representative of aerosol impacts on convection in other regions of the world or of the impacts of other aerosol types.

For the purposes of this study, we chose only two environmental factors (CAPE and LTSS) with which to stratify the data. Both of these parameters are bulk parameters that provide significant information about the environment in which storms form. However, it is impossible to entirely rule out the role of the environment, as other factors can also be important. For instance, *Khain et al.* [2008] showed that the relative humidity can be a factor in determining the response of DCCs to aerosol concentrations, particularly the precipitation response. In addition, other studies [*Lee et al.*, 2008b; *Fan et al.*, 2009] have demonstrated that strong wind shear can suppress deep convective clouds in the presence of high aerosol concentrations, a hypothesis which we did not examine here. Analyzing other environmental factors such as these is important work that would be useful for future study.

In this study, we have established that there is indeed a significant relationship between aerosol optical depth and bulk cloud parameters including cloud top, rain top, and center of gravity. In the future, the combination of satellite data and model output may be used in the manner demonstrated here to examine the problem in more detail. For instance, by utilizing aerosol optical depth, we have neglected information about specific aerosol size and type, as well as the vertical distribution of aerosols in the atmosphere. It may be useful to separate the larger dust aerosols from the smaller sulfate particles, for instance, in order to better understand the mechanisms leading to changes in cloud parameters. It would also be interesting

to look at any differences that may arise due to the vertical distribution of aerosols. Aerosol particles may be ingested into a storm updraft at the cloud base or entrained at midlevels; however, little is known about the relative importance of those two mechanisms.

We have shown here that there exists significant evidence that aerosols in the east Atlantic are affecting deep convective clouds through the processes of convective invigoration.

Acknowledgments
Data used for this research can be obtained from the CloudSat Data Processing Center (http://www.cloudsat.cira.colostate.edu/dataHome.php), and ECMWF (http://apps.ecmwf.int/datasets/). This work was funded by the National Science Foundation under grant NSFATM-0820557. The authors would like to thank Matthew Lebsock for providing GEMS model data matched to CloudSat profiles. Thank you also to the three anonymous reviewers whose input helped to improve this work.

References

Andreae, M., D. Rosenfeld, P. Artaxo, A. Costa, G. Frank, K. Longo, and M. Silva-Dias (2004), Smoking rain clouds over the Amazon, *Science*, *303*, 1337–1342.

Austin, R. T., A. J. Heymsfield, and G. L. Stephens (2009), Retrieval of ice cloud microphysical parameters using the CloudSat millimeter-wave radar and temperature, *J. Geophys. Res.*, *114*, D00A23, doi:10.1029/2008JD010049.

Bell, T. L., D. Rosenfeld, K.-M. Kim, J.-M. Yoo, M.-I. Lee, and M. Hahnenberger (2008), Midweek increase in U.S. summer rain and storm heights suggests air pollution invigorates rainstorms, *J. Geophys. Res.*, *113*, D02209, doi:10.1029/2007JD008623.

Benedetti, A., et al. (2009), Aerosol analysis and forecast in the European Centre for Medium-Range Weather Forecasts Integrated Forecast System: 2. Data assimilation, *J. Geophys. Res.*, *114*, D13205, doi:10.1029/2008JD011115.

Carlson, T. N., and J. M. Prospero (1972), The large-scale movement of Saharan air outbreaks over the northern equatorial Atlantic, *J. Appl. Meteorol.*, *11*, 283–297.

DeMott, P. J., K. Sassen, M. R. Poellot, D. Baumgardner, D. C. Rogers, S. D. Brooks, A. J. Prenni, and S. M. Kreidenweis (2003), African dust aerosols as atmospheric ice nuclei, *Geophys. Res. Lett.*, *30*(14), 1732, doi:10.1029/2003GL017410.

Durden, S. L., S. Tanelli, and G. Dobrowski (2009), CloudSat and A-Train observations of tropical cyclones, *Open Atmos. Sci. J.*, *3*, 80–92.

Fan, J., T. Yuan, J. M. Comstock, S. Ghan, A. Khain, L. R. Leung, Z. Li, V. J. Martins, and M. Ovchinnikov (2009), Dominant role by vertical wind shear in regulating aerosol effects on deep convective clouds, *J. Geophys. Res.*, *114*, D22206, doi:10.1029/2009JD012352.

Fan, J., D. Rosenfeld, Y. Din, L. R. Leung, and Z. Li (2012), Potential aerosol indirect effects on atmospheric circulation and radiative forcing through deep convection, *Geophys. Res. Lett.*, *39*, L09806, doi:10.1029/2012GL051851.

Fan, J., L. R. Leung, D. Rosenfeld, Q. Chen, Z. Li, J. Zhang, and H. Yan (2013), Microphysical effects determine macrophysical response for aerosol impacts on deep convective clouds, *Proc. Natl. Acad. Sci. U.S.A.*, *110*, E4581–E4590.

Haynes, J. M., T. S. L'Ecuyer, G. L. Stephens, S. D. Miller, C. Mitrescu, N. B. Wood, and S. Tanelli (2009), Rainfall retrieval over the ocean with spaceborne W-band radar, *J. Geophys. Res.*, *114*, D00A22, doi:10.1029/2008JD009973.

Heiblum, R. H., I. Koren, and O. Altaratz (2012), New evidence of cloud invigoration from TRMM measurements of rain center of gravity, *Geophys. Res. Lett.*, *39*, L08803, doi:10.1029/2012GL051158.

Hollingsworth, A., et al. (2008), Toward a monitoring and forecasting system for atmospheric composition, *Bull. Am. Meteorol. Soc.*, *89*, 1147–1164.

Khain, A. (2009), Notes on state-of-the-art investigations of aerosol effects on precipitation: A critical review, *Environ. Res. Lett.*, *4*, 015004.

Khain, A., D. Rosenfeld, and A. Pokrovsky (2005), Aerosol impact on the dynamics and microphysics of deep convective clouds, *Q. J. R. Meteorol. Soc.*, *131*, 2639–2664.

Khain, A., N. BenMoshe, and A. Pokrovsky (2008), Factors determining the impact of aerosols on surface precipitation from clouds: An attempt at classification, *J. Atmos. Sci.*, *65*, 1721–1748.

Khain, A., D. Rosenfeld, A. Pokrovsky, U. Blahak, and A. Ryzhkov (2010), The role of CCN in precipitation and hail in a mid-latitude storm as seen in simulations using a spectral (bin) microphysics model in a 2D dynamic frame, *Atmos. Res.*, *99*, 129–146.

Koren, I., Y. J. Kaufman, D. Rosenfeld, L. A. Remer, and Y. Rudich (2005), Aerosol invigoration and restructuring of Atlantic convective clouds, *Geophys. Res. Lett.*, *32*, L14828, doi:10.1029/2005GL023187.

Koren, I., O. Altaratz, G. Feingold, Z. Levin, and T. Reisin (2009), Cloud's center of gravity—A compact approach to analyze convective cloud development, *Atmos. Chem. Phys.*, *9*, 155–161.

Lebo, Z. J., and J. H. Seinfeld (2011), Theoretical basis for convective invigoration due to increased aerosol concentration, *Atmos. Chem. Phys.*, *11*, 2773–2842.

Lee, S. S., L. J. Donner, V. T. J. Phillips, and Y. Ming (2008a), Examination of aerosol effects on precipitation in deep convective clouds during the 1997 ARM summer experiment, *Q. J. R. Meteorol. Soc.*, *134*, 1201–1220.

Lee, S. S., L. J. Donner, V. T. J. Phillips, and Y. Ming (2008b), The dependence of aerosol effects on clouds and precipitation on cloud-system organization, shear and stability, *J. Geophys. Res.*, *113*, D16202, doi:10.1029/2007JD009224.

Li, G., Y. Wang, and R. Zhang (2008), Implementation of a two-moment bulk microphysics scheme to the WRF model to investigate aerosol-cloud interaction, *J. Geophys. Res.*, *113*, D15211, doi:10.1029/2007JD009361.

Li, Z., F. Niu, J. Fan, Y. Liu, D. Rosenfeld, and Y. Ding (2011), Long-term impacts of aerosols on the vertical development of clouds and precipitation, *Nat. Geosci.*, *4*, 888–894.

Lin, J. C., T. Matsui, R. A. Pielke Sr., and C. Kummerow (2006), Effects of biomass-burning-derived aerosols on precipitation and clouds in the Amazon Basin: A satellite-based empirical study, *J. Geophys. Res.*, *111*, D19204, doi:10.1029/2005JD006884.

Liu, C., E. Zipser, and S. Nesbitt (2007), Global distribution of tropical deep convection: Different perspectives from TRMM infrared and radar data, *J. Clim.*, *20*, 489–503.

Luo, Z., G. Y. Liu, G. L. Stephens, and R. H. Johnson (2009), Terminal versus transient cumulus congestus: A CloudSat perspective, *Geophys. Res. Lett.*, *36*, L05808, doi:10.1029/2008GL036927.

Lynn, B., A. Khain, J. Dudhia, D. Rosenfeld, A. Pokrovsky, and A. Seifert (2005), Spectral (bin) microphysics coupled with a mesoscale model (MM5). Part II: Simulation of a CaPE rain event with a squall line, *Mon. Weather Rev.*, *133*, 59–71.

Mace, G. G., R. Marchand, Q. Zhang, and G. Stephens (2007), Global hydrometeor occurrence as observed by CloudSat: Initial observations from summer 2006, *Geophys. Res. Lett.*, *34*, L09808, doi:10.1029/2006GL029017.

Matsui, T., H. Masunaga, R. A. Pielke Sr., and W.-K. Tao (2004), Impact of aerosols and atmospheric thermodynamics on cloud properties within the climate system, *Geophys. Res. Lett.*, *31*, L06109, doi:10.1029/2003GL019287.

Min, Q. L., R. Li, B. Lin, E. Joseph, S. Wang, Y. Hu, V. Morris, and F. Chang (2009), Evidence of mineral dust altering cloud microphysics and precipitation, *Atmos. Chem. Phys.*, *9*, 3223–3231.

Protat, A., D. Bouniol, J. Delanoe, E. O'Connor, P. T. May, A. Plana-Fattori, A. Hasson, U. Gorsdorf, and A. J. Heymsfield (2009), Assessment of CloudSat reflectivity measurements and ice cloud properties using ground-based and airborne cloud radar observations, *J. Atmos. Oceanic Technol.*, *26*, 1717–1741.

Remer, L., Y. Kaufman, and D. Tanré (2005), The MODIS aerosol algorithm, products, and validation, *J. Atmos. Sci.*, *62*, 947–973.
Remer, L. A., et al. (2008), Global aerosol climatology from the MODIS satellite sensors, *J. Geophys. Res.*, *113*, D14S07, doi:10.1029/2007JD009661.
Rosenfeld, D., U. Lohmann, G. Raga, C. O'Dowd, M. Kulmala, S. Fuzzi, A. Reissell, and M. Andreae (2008), Flood or drought: How do aerosols affect precipitation?, *Science*, *321*, 1309–1313.
Stephens, G., et al. (2002), The CloudSat mission and the A-Train: A new dimension to space-based observations of clouds and precipitation, *Bull. Am. Meteorol. Soc.*, *83*, 1771–1790.
Storer, R. L., and S. C. van den Heever (2013), Microphysical processes evident in aerosol forcing of tropical deep convective clouds, *J. Atmos. Sci.*, *70*, 430–446.
Storer, R. L., S. C. van den Heever, and G. L. Stephens (2010), Modeling aerosol impacts on convective storms in different environments, *J. Atmos. Sci.*, *67*, 3904–3915.
Tao, W.-K., J.-P. Chen, Z. Li, C. Wang, and C. Zhang (2012), Impact of aerosols on convective clouds and precipitation, *Rev. Geophys.*, *50*, RG2001, doi:10.1029/2011RG000369.
Ten Hoeve, J. E., M. Z. Jacobson, and L. A. Remer (2012), Comparing results from a physical model with satellite and in situ observations to determine whether biomass burning aerosols over the Amazon brighten or burn off clouds, *J. Geophys. Res.*, *117*, D08203, doi:10.1029/2011JD016856.
Twohy, C. H., et al. (2009), Saharan dust particles nucleate droplets in eastern Atlantic clouds, *Geophys. Res. Lett.*, *36*, L01807, doi:10.1029/2008GL035846.
van den Heever, S., and W. Cotton (2007), Urban aerosol impacts on downwind convective storms, *J. Appl. Meteorol. Climatol.*, *46*, 828–850.
van den Heever, S., G. Carrió, W. Cotton, P. DeMott, and A. Prenni (2006), Impacts of nucleating aerosol on Florida storms. Part I: Mesoscale simulations, *J. Atmos. Sci.*, *63*, 1752–1775.
van den Heever, S. C., G. L. Stephens, and N. B. Wood (2011), Aerosol indirect effects on tropical convection characteristics under conditions of radiative–convective equilibrium, *J. Atmos. Sci.*, *68*, 699–718.
Wang, J., S. C. van den Heever, and J. S. Reid (2009), A conceptual model for the link between Central American biomass burning aerosols and severe weather over the south central United States, *Environ. Res. Lett.*, *4*, 015003.
Wang, Y., Q. Wan, W. Meng, F. Liao, H. Tan, and R. Zhang (2011), Long-term impacts of aerosols on precipitation and lightning over the Pearl River Delta megacity area in China, *Atmos. Chem. Phys.*, *11*, 12,421–12,436.
Wilks, D. (2006), *Statistical Methods in the Atmospheric Sciences, Int. Geophys. Ser.*, vol. 59, 2nd ed., Academic Press, Burlington, MA.
Yuter, S., and R. Houze (1995), Three-dimensional kinematic and microphysical evolution of Florida cumulonimbus. Part II: Frequency distributions of vertical velocity, reflectivity, and differential reflectivity, *Mon. Weather Rev.*, *123*, 1941–1963.
Zipser, E. J., et al. (2009), The Saharan air layer and the fate of African easterly waves—NASA's AMMA field study of tropical cyclogenesis, *Bull. Am. Meteorol. Soc.*, *90*, 1137–1156.